Journal of Lasers in Medical Sciences

J Lasers Med Sci 2023;14:e60

Original Article

http://journals.sbmu.ac.ir/jlms

doi 10.34172/jlms.2023.60

Efficacy Evaluation of Human Skin Treatment with Photodynamic Therapy in Actinic Keratoses Patients

Zahra Razzaghi[1], Babak Arjmand[2], Maryam Hamzeloo-Moghadam[3], Mostafa Rezaei Tavirani[4*], Mona Zamanian Azodi[4]

[1]Laser Application in Medical Sciences Research Center, Shahid Beheshti University of Medical Sciences, Tehran, Iran
[2]Cell Therapy and Regenerative Medicine Research Center, Endocrinology and Metabolism Molecular-Cellular Sciences Institute, Tehran University of Medical Sciences, Tehran, Iran
[3]Traditional Medicine and Materia Medica Research Center, School of Traditional Medicine, Shahid Beheshti University of Medical Sciences, Tehran, Iran
[4]Proteomics Research Center, Faculty of Paramedical Sciences, Shahid Beheshti University of Medical Sciences, Tehran, Iran

***Correspondence to**
Mostafa Rezaei Tavirani,
Email: tavirany@yahoo.com

Received: September 9, 2023
Accepted: October 15, 2023
ePublished: November 29, 2023

Abstract

Introduction: Photodynamic therapy (PDT) is a combined method of light and light-activated chemicals that are called photosensitizers (PSs). PDT is recommended as a high cure rate method with fewer side effects and a noninvasive tool to treat cancer. This study aimed to evaluate PDT efficacy as a therapeutic method against actinic keratoses in patients via protein-protein interaction (PPI) network analysis by using the gene expression profiles of Gene Expression Omnibus (GEO).

Methods: Twenty-one gene expression profiles were extracted from GEO and analyzed by GEO2R to determine the significant differentially expressed genes (DEGs). The significant DEGs were included in PPI networks via Cytoscape software. The networks were analyzed by the "Network Analyzer", and the elements of the main connected components were assessed.

Results: There were three main connected components for the compared sets of the gene expression profiles including the lesional region of skin before (Before set) and after (After set) PDT versus healthy (healthy set) skin and before versus after. The before-health comparison showed a partial similarity with the After-Healthy assessment. The before-after evaluation indicated that there were not considerable differences between the gene expression profile of the lesional region before and after PDT.

Conclusion: In conclusion, PDT was unable to return the gene expression pattern of the actinic keratoses skin to a healthy condition completely.

Keywords: Photodynamic therapy; PPI network; Human skin; Actinic keratoses; Gene expression.

Introduction

Photodynamic therapy (PDT) is a combined method including light and light-activated chemicals which are known as PSs. PDT is a photochemical-based treatment method. Achieving a suitable PS is a critical goal in PDT because the role of PSs in producing photoinduced reactive oxygen species (ROS) is an essential process in PDT. It is expressed that application of PS in PDT is improved. It is highlighted that PDT is associated with fewer side effects and high cure rates. The noninvasive nature of PDT is pointed out in many documents. It is predicted that PDT can be considered a suitable candidate for alternative conventional cancer treatments.[1-3]

Gene expression analysis as a useful tool is applied to explore the details of the molecular mechanism of many diseases and clinical methods. The assessment of cancer initiation, development, and treatment is strongly concerned with gene expression evaluation. In such an investigation, the gene expression profiles of the cancerous samples before and after treatment are analyzed and the details of response to treatment based on the alterations of gene expression in the related genes are determined.[4-6]

Bioinformatics as a developed science has attracted many researchers' attention in biology and medicine. Many diseases have been investigated via bioinformatic tools. Protein-protein interaction (PPI) network analysis has occupied a unique situation in bioinformatics and is applied to explore the molecular mechanism of numerous diseases. Since bioinformatics is a well-known approach for the assessment of high throughput data, gene expression analysis is tied to bioinformatics and network analysis.[7-10] A large number of dysregulated genes are organized in the interacted unit as a network, and each gene will interact with the related neighbors in a certain mode. The PPI network is a strong tool for screening the assessed genes. PPI network analysis is used widely to

Please cite this article as follows: Razzaghi Z, Arjmand B, Hamzeloo-Moghadam M, Rezaei Tavirani M, Zamanian Azodi M. Efficacy evaluation of human skin treatment with photodynamic therapy in actinic keratoses patients. *J Lasers Med Sci*. 2023;14:e60. doi:10.34172/jlms.2023.60.

detect molecular events after radiation. There are many valuable investigations about laser therapy which are administrated via PPI network analysis.[11,12] In the present study, the gene expression profiles of actinic keratoses before and after applying PDT relative to the healthy skin of patients[13] were extracted from Gene Expression Omnibus (GEO) (https://www.ncbi.nlm.nih.gov/geo/query/acc.cgi?acc=gse90643), and the efficacy of the treatment method was evaluated via network analysis.

Methods

Data Collection

The gene expression profiles of seven patients with actinic keratosis, which are treated with PDT with topical methyl aminolevulinate (MAL) treatment, were extracted from GSE90643 which is recorded in the GEO. Three biopsy samples of each patient, including the healthy skin areas before treatment, the lesional region before treatment, and the lesional regions after 18 weeks of treatment were selected for analysis. Three analyses for drawing a comparison between the gene expression profiles were planned; before - Healthy (the lesional region before treatment-healthy skin areas before treatment), before-After (the lesional region before treatment-the lesional region after 18 weeks of treatment), and After-Healthy (the lesional region after 18 weeks of treatment-healthy skin areas before treatment).

Pre-evaluation of Data

In the first step, analyses were assessed via GEO2R to detect significant differentially expressed genes (DEGs) which discriminate the two evaluated sets of gene expression profiles. The results of investigations are presented as volcano plots and box plots. 250 top DEGs (based on $P_{adjust} < 0.05$) were chosen for analysis. The selected DEGs were screened based on (fold change) ≥ 2. Among the DEGs that were characterized by more than one value of expression, the most fold change value was considered.

Network Analysis

The screened significant DEGs were included in the "Protein Query" of the STRING database to form PPI networks via Cytoscape software v 3.7.2. The PPI networks were constructed by the recognized significant DEGs by the STRING database. The PPI networks were analyzed by the "Network Analyzer" application of Cytoscape software to find the pattern of node organization in the networks. The main connected component (the largest sub-network in each analysis) of the networks was determined and analyzed to find the critical genes (the nodes with a higher value of connections).

Statical Analysis

The statistical analysis of the examination was based on the following criteria: Fold change > 2 $P_{adjust} < 0.05$, Confidence score = 0.4.

Results

The volcano plot and the box plot for the BEFORE-HEALTHY ANALYSIS are shown in Figures 1-2. Based on the volcano plot pattern, there are many DEGs that discriminate the two sets of the compared gene expression profiles. As shown in the box plot, all gene expression profiles are characterized by similar median points and are comparable. A PPI network including 169 recognized DEGs, 77 isolated genes, 16 paired nodes, three triples, one pentad, and a main connected component (containing 62 nodes) was constructed. Due to the importance of the main connected component as the largest sub-network, it is presented in Figure 3. Centrality parameters such as

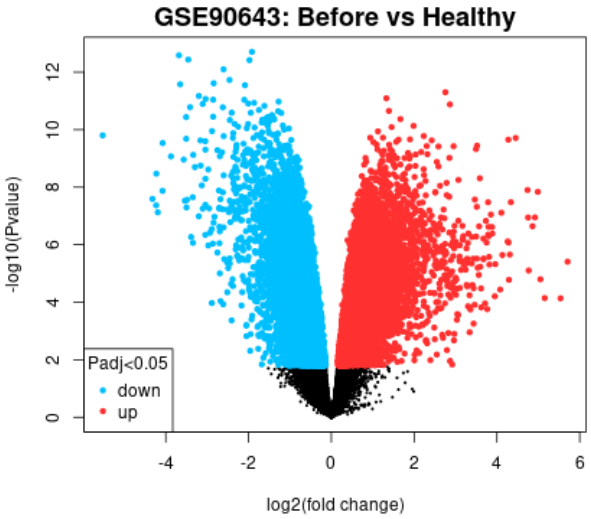

Figure 1. Volcano Plot of Before-Healthy Analysis. Distribution of normalized amounts of expression as the function of log (fold change) is presented

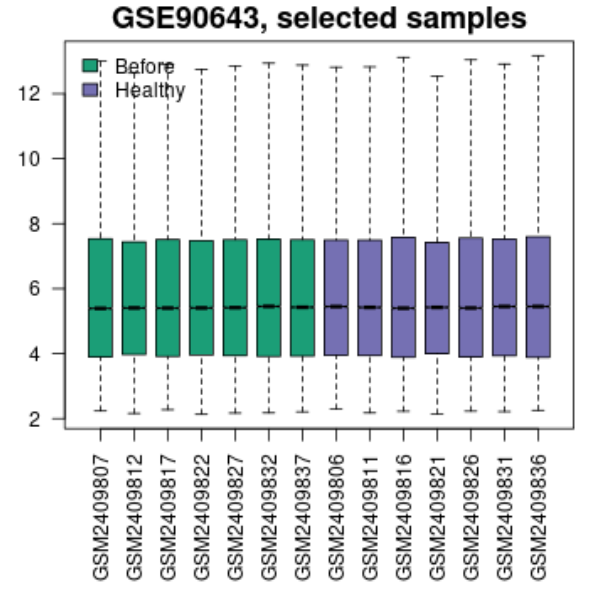

Figure 2. Box Plot of Before-Healthy Analysis. Distribution of the normalized amounts of expression is presented for samples

degree value and betweenness centrality were determined for the nodes of the main connected component of the analyzed network (see Table 1).

The results of the before-after gene expression profile analysis as the volcano plot and the box plot are presented in Figures 4-5. Similar to the analysis of before-healthy, the box plot finding indicates the possible comparison between the evaluated gene expression profiles, but a different volcano plot appears. Based on the volcano plot, a limited number of significant DEGs are identified. The PPI network is formed from 55 recognized significant DEGs including 17 isolated nodes, 8 paired genes, and a main connected component of 30 DEGs (see Figure 6 and Table 2).

After-healthy gene expression profiles were compared, and the related volcano plot and box plot were provided (see Figures 7-8). The presented volcano plot and box plot for After-Healthy analysis are similar to the before-healthy individual and differ from the before-after one (considering the volcano plot). This means there are considerable differences between the treated samples and the control individuals. 149 queried significant DEGs were recognized by the STRING database and formed the PPI network. The network included 67 isolated genes, eight paired genes, four triples, two tetrads, and a main connected component (containing 54 nodes). The main connected component and its related nodes are shown in Figure 9 and Table 3.

Discussion

Padilla et al have reported a document about the essential

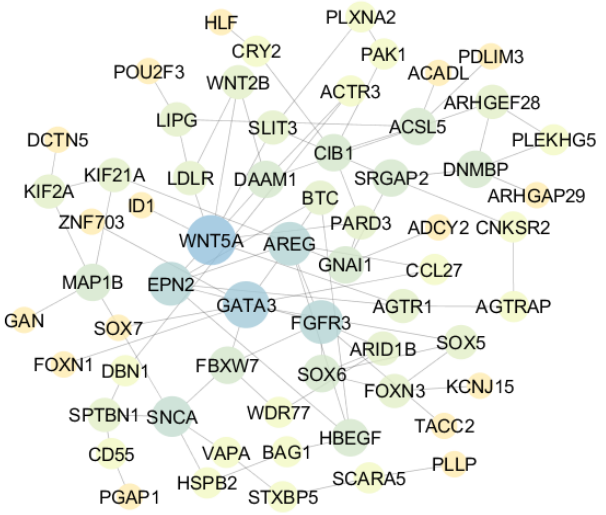

Figure 3. Main Connected Component of the PPI Network of Before-Healthy Analysis. Nodes are layout based on degree value. The bigger size of nodes refers to an increase in the degree

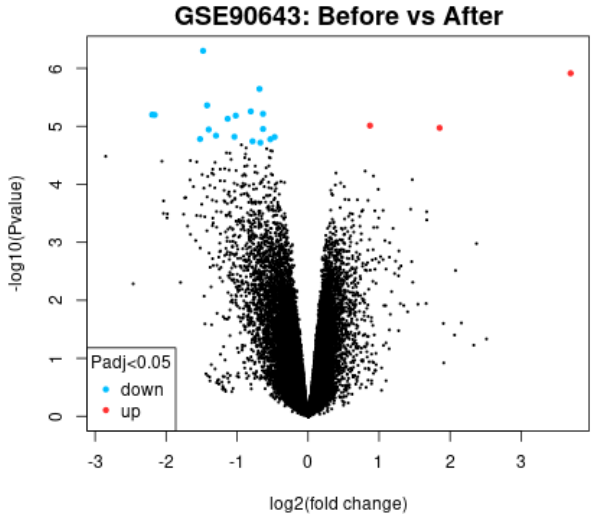

Figure 4. Volcano Plot of Before-After Analysis. Distribution of the normalized amounts of expression as the function of log(fold change) is presented

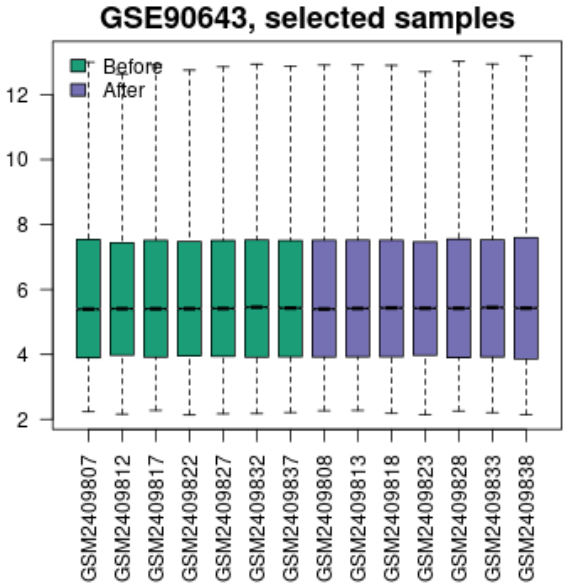

Figure 5. Box Plot of Before-After Analysis. Distribution of the normalized amounts of expression is presented for the samples

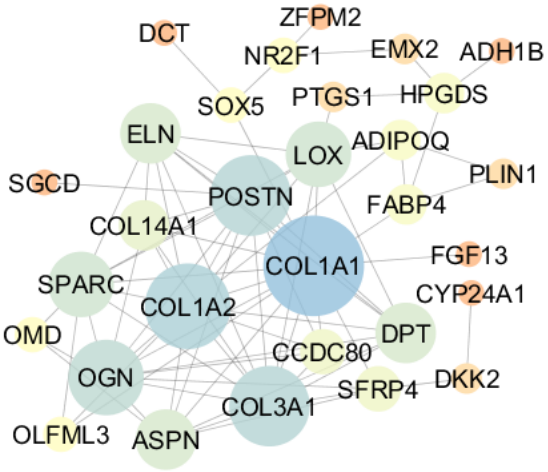

Figure 6. Main Connected Component of the PPI Network of Before-After Analysis. Nodes are layout based on degree value. The bigger size of nodes refers to an increase in the degree

Table 1. Centrality Parameters of Nodes of the Main Connected Component of the PPI Network of Before-Healthy Analysis

R	Display Name	Degree	Betweenness Centrality
1	WNT5A	8	0.38
2	GATA3	7	0.14
3	AREG	6	0.11
4	EPN2	6	0.31
5	FGFR3	6	0.2
6	SNCA	5	0.27
7	ACSL5	4	0.08
8	CIB1	4	0.14
9	DAAM1	4	0.12
10	DNMBP	4	0.05
11	FBXW7	4	0.17
12	GNAI1	4	0.17
13	HBEGF	4	0.04
14	MAP1B	4	0.15
15	SOX6	4	0.06
16	SRGAP2	4	0.09
17	AGTR1	3	0.04
18	ARHGEF28	3	0.04
19	ARID1B	3	0.01
20	BTC	3	0
21	FOXN3	3	0.03
22	KIF21A	3	0.12
23	KIF2A	3	0.03
24	LDLR	3	0.08
25	LIPG	3	0.06
26	PARD3	3	0.2
27	SLIT3	3	0.07
28	SOX5	3	0.02
29	SPTBN1	3	0.1
30	WNT2B	3	0.01
31	ACTR3	2	0.06
32	AGTRAP	2	0.01
33	BAG1	2	0.02
34	CCL27	2	0
35	CD55	2	0.03
36	CNKSR2	2	0.01
37	CRY2	2	0.03
38	DBN1	2	0.05
39	HSPB2	2	0.02
40	PAK1	2	0.01
41	PLEKHG5	2	0
42	PLXNA2	2	0.01
43	SCARA5	2	0.03
44	STXBP5	2	0.06
45	VAPA	2	0.1
46	WDR77	2	0
47	ACADL	1	0
48	ADCY2	1	0
49	ARHGAP29	1	0
50	DCTN5	1	0
51	FOXN1	1	0
52	GAN	1	0
53	HLF	1	0
54	ID1	1	0
55	KCNJ15	1	0
56	PDLIM3	1	0
57	PGAP1	1	0
58	PLLP	1	0
59	POU2F3	1	0
60	SOX7	1	0
61	TACC2	1	0
62	ZNF703	1	0

Table 2. Centrality Parameters of the Elements of the Main Connected Component of the PPI Network of Before-After Analysis

R	Display Name	Degree	Betweenness Centrality
1	COL1A1	16	0.48
2	COL1A2	13	0.06
3	COL3A1	12	0.04
4	POSTN	12	0.08
5	OGN	11	0.04
6	LOX	9	0.10
7	SPARC	9	0.03
8	ASPN	8	0.03
9	DPT	8	0.00
10	ELN	8	0.00
11	COL14A1	6	0.00
12	CCDC80	5	0.00
13	SFRP4	5	0.13
14	ADIPOQ	4	0.03
15	FABP4	4	0.15
16	HPGDS	4	0.12
17	NR2F1	3	0.10
18	OLFML3	3	0.00
19	OMD	3	0.00
20	SOX5	3	0.19
21	DKK2	2	0.07
22	EMX2	2	0.03
23	PLIN1	2	0.00
24	PTGS1	2	0.03
25	ADH1B	1	0.00
26	CYP24A1	1	0.00
27	DCT	1	0.00
28	FGF13	1	0.00
29	SGCD	1	0.00
30	ZFPM2	1	0.00

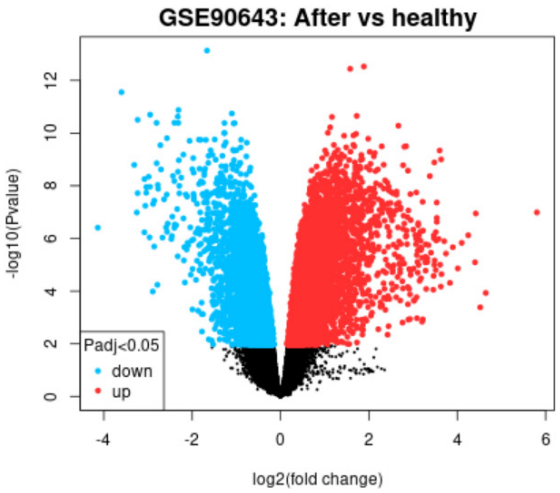

Figure 7. Volcano Plot of the After-Healthy Analysis. Distribution of the normalized amounts of expression as the function of log(fold change) is presented

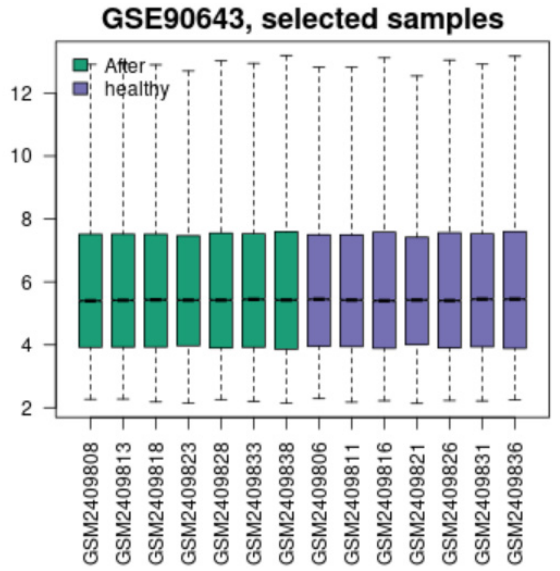

Figure 8. Box Plot of the After-Healthy Analysis. Distribution of the normalized amounts of expression is presented for the samples

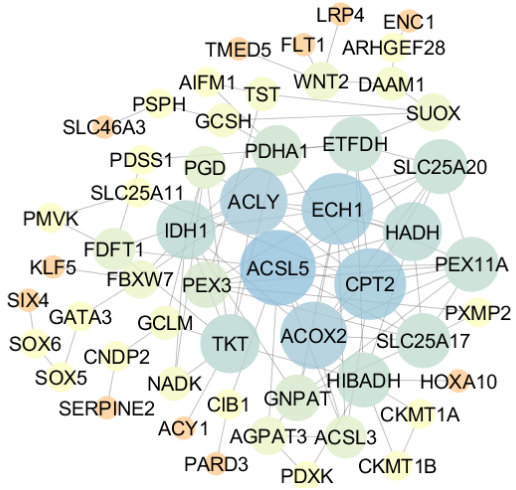

Figure 9. Main Connected Component of the After-Healthy PPI Network. Nodes are layout based on degree value. The bigger size of nodes refers to an increase in the degree

differences between the gene expression pattern of human actinic keratosis and normal skin.[14] As shown in Figure, 1,2, the gene expression profiles of before-healthy skin samples are comparable and characterized by many DEGs. Volcano plot analysis indicates that there are many significantly dysregulated genes which discriminate the lesional region from healthy skin. Various types of genes among the identified DEGs were recognized by the STRING database. Among 169 recognized DEGs, 62 individuals formed a main sub-network (see Figure 3). In the present study, it is proposed that nodes of this sub-network are the critical DEGs, which differentiate healthy and lesional regions of the skin. The roles of the nodes in the sub-network are determined based on centrality parameters. More details are shown in Table 1. The 5 top DEGs (based on degree value) in Table 1 are WNT5A, GATA3, AREG, EPN2, and FGFR3. Ra et al have published data about the role of WNT5A as a discriminator gene that differentiates cutaneous squamous cell carcinoma from actinic keratosis and normal skin.[15] WNT5A is the first ranked gene in Table 1. Solus et al have reported that GATA3 immunohistochemical staining decreases in cutaneous squamous cell carcinoma.[16] Log (fold change) of GATA3 in the GSE90643 is recorded as -1.853 for lesional region - healthy skin comparison. As shown in Table 1, GATA3 is ranked as the second top gene. The results indicate that there is a unique molecular signature that differentiates the lesional region from healthy skin before PDT.

Due to the application of PDT for the treatment of large areas, it is introduced as a suitable therapy for non-melanoma skin cancers such as actinic keratoses.[17] Piaserico et al have published an evidence-based review about combination-based strategies to apply PDT as a tool for the treatment of actinic keratoses.[18] It can be expected that PDT leads to omitting the gene expression differences between the lesional region after the treatment and healthy skin. It can be concluded that the results of the before-after analysis should be similar to the findings of the before-healthy assessment. As it is depicted in Figure 5, before-after analysis like before-healthy assessment is possible statistically. The comparison of Figures 1 and 4 indicates that there are essential differences between the volcano plots of both before-healthy and before-After analyses. Ranges of fold change and *P* value changes for the before-after analysis relative to before-healthy are limited. It means that the gene expression profiles of the "lesional region before treatment" after PDT change moderately. Comparison of Figure 3 and Table 1 with Figure 6 and Table 2 confirms the findings. The main connected component of the before-healthy analysis is characterized by 62 nodes while the

Table 3. Centrality Parameters of Nodes of the Main Connected Component of the After-Healthy PPI Network

R	Display Name	Degree	Betweenness Centrality
1	ACSL5	13	0.13
2	CPT2	12	0.10
3	ECH1	12	0.07
4	ACLY	11	0.19
5	ACOX2	11	0.04
6	HADH	9	0.04
7	IDH1	9	0.12
8	TKT	9	0.17
9	ETFDH	8	0.23
10	HIBADH	8	0.16
11	PEX11A	8	0.00
12	SLC25A17	8	0.02
13	SLC25A20	8	0.02
14	PDHA1	7	0.17
15	GNPAT	6	0.02
16	PEX3	6	0.04
17	ACSL3	5	0.00
18	FDFT1	5	0.05
19	PGD	5	0.02
20	AGPAT3	4	0.01
21	FBXW7	4	0.18
22	SUOX	4	0.25
23	WNT2	4	0.11
24	DAAM1	3	0.21
25	GCLM	3	0.07
26	GCSH	3	0.10
27	NADK	3	0.00
28	TST	3	0.03
29	AIFM1	2	0.01
30	ARHGEF28	2	0.04
31	CIB1	2	0.04
32	CKMT1A	2	0.00
33	CKMT1B	2	0.00
34	CNDP2	2	0.04
35	GATA3	2	0.11
36	PDSS1	2	0.01
37	PDXK	2	0.00
38	PMVK	2	0.00
39	PSPH	2	0.04
40	PXMP2	2	0.00
41	SLC25A11	2	0.01
42	SOX5	2	0.07
43	SOX6	2	0.04
44	ACY1	1	0.00
45	ENC1	1	0.00
46	FLT1	1	0.00
47	HOXA10	1	0.00
48	KLF5	1	0.00
49	LRP4	1	0.00
50	PARD3	1	0.00
51	SERPINE2	1	0.00
52	SIX4	1	0.00
53	SLC46A3	1	0.00
54	TMED5	1	0.00

before-after assessment is branded with a main connected component of 30 DEGs. As it is shown in Tables 1 and 2, SOX5 is the only common DEGs for the two compared main connected components of PPI networks of before-healthy and before-after analyses. SRY-box (SOX) is a protein family including more than 20 transcription factors such as SOX1 and SOX2, which play roles in tumor and metastasis.[19] Investigations indicate that SOX5 participates in the life cycle regulation of melanocytes.[20] SOX1 appears as a common DEG between both analyses, and it is over-expressed in the lesional region before and after PDT application versus healthy skin. Yuan et al have introduced SOX5 as a suppressor factor for Kaposi's sarcoma.[21] It can be concluded that SOX5 is over-expressed in response to skin damage. This conclusion is consistent with the up-regulation (fold change is about 9) of SOX5 in the lesional region before the treatment versus healthy skin. It is predictable that PDT leads to a decrease in damages. SOX2 is down-regulated (fold change is about 2.5) in the lesional region after PDT treatment. However, PDT has reduced the SOX5 level in the lesional region, and it seems the pathological molecular events are controlled partially because the elevated level of SOX1 in the tissue before PDT is at least 3 times bigger than the modified value of SOX5 level in the lesional region after the treatment. On the other hand, there are significant differences between healthy skin and the lesional region of skin which is treated with PDT.

For more resolution, the results of after-healthy analysis are presented in Figures 7-9 and Table 3. Like the two performed analyses, this evaluation is possible due to the comparable presented gene expression profiles in Figure 8. Surprisingly, the volcano plots of both Before-Health and After-Healthy analyses are similar (see Figures 1 and 7), while the volcano plots of After-Healthy and after-Before are different (comparison of Figures 7 and 4). The similarity between Figures 9 and 3, which is confirmed by the comparison of Tables 1 and 3, corresponds to the similarity of the gene expression profiles of the lesional region of skin before and after applying PDT.

There are 9 common DEGs (including SOX5, SOX6, PARD3, GATA3, FBXW7, DAAM1, CIB1, ARHGEF28, and ACSL5) for main connected components of After-Healthy and Before-Healthy analyses. It can be concluded that applying PDT was not able to return the gene expression pattern of the lesional region of the skin to a healthy condition, but it may have reduced the signs of damages. Joly et al reported that the abnormal proliferation-related gene profiles and expressed cancer-associated genes in the actinic keratoses patients were corrected by MAL-PDT treatment.[13] Jerjes et al treated 147 consecutive patients with oral potentially malignant disorders by surface illumination PDT, using 5-ALA or mTHPC as the photosensitizer. Results indicated that 81% of the patients were treated completely. In this report, PDT is recommended as an efficient therapeutic method with fewer side effects.[22] Time of administration and associated pain are pointed out as the main disadvantages of PDT.[23] Nevertheless, several significant weaknesses are counted for the clinical application of PDT: First, PDT is oxygen-dependent; second, the remained PSs make skin and normal tissues sensitive to light, and third, strong aggregation of the conjugated hydrophobic PSs forms in aqueous solutions.[24] Due to the complex features of the findings, more investigations into the application and approvement of PDT are required.

Conclusion

In conclusion, PDT as a safe method has attracted the attention of experts to fight against accessible cancers. Our finding revealed the complex molecular mechanism of PDT. However, PDT inhibited actinic keratoses, and there were differences between the gene expression profiles of the lesional region of the skin before and after the treatment. It means that the treated samples contain additional alterations in gene expression and function.

Authors' Contribution

Conceptualization: Babak Arjmand, Mostafa Rezaei Tavirani.
Data curation: Mona Zamanian Azodi.
Formal analysis: Mostafa Rezaei Tavirani.
Funding acquisition: Mostafa Rezaei Tavirani.
Investigation: Mona Zamanian Azodi, Maryam Hamzeloo-Moghadam.
Methodology: Mona Zamanian Azodi, Zahra Razzaghi.
Project administration: Babak Arjmand, Mostafa Rezaei Tavirani.
Resources: Zahra Razzaghi.
Software: Zahra Razzaghi, Mona Zamanian Azodi.
Supervision: Mostafa Rezaei Tavirani, Maryam Hamzeloo-Moghadam.
Validation: Zahra Razzaghi.
Visualization: Mona Zamanian Azodi.
Writing–original draft: Mostafa Rezaei Tavirani, Mona Zamanian Azodi.
Writing–review & editing: Babak Arjmand, Zahra Razzaghi, Maryam Hamzeloo-Moghadam.

Competing Interests

The authors declare they have no conflicts of interest.

Ethical Approval

This project was approved by Shahid Beheshti University of Medical Sciences with the ethical code of IR.SBMU.LASER.REC.1402.012.

Funding

Shahid Beheshti University of Medical Sciences supported this research.

References

1. Pham TC, Nguyen VN, Choi Y, Lee S, Yoon J. Recent strategies to develop innovative photosensitizers for enhanced photodynamic therapy. Chem Rev. 2021;121(21):13454-619. doi: 10.1021/acs.chemrev.1c00381.
2. Li X, Lovell JF, Yoon J, Chen X. Clinical development and potential of photothermal and photodynamic therapies for cancer. Nat Rev Clin Oncol. 2020;17(11):657-74. doi: 10.1038/s41571-020-0410-2.
3. Lo PC, Rodríguez-Morgade MS, Pandey RK, Ng DKP, Torres T, Dumoulin F. The unique features and promises of phthalocyanines as advanced photosensitisers for photodynamic therapy of cancer. Chem Soc Rev. 2020;49(4):1041-56. doi: 10.1039/c9cs00129h.
4. Suh HY, Choi H, Paeng JC, Cheon GJ, Chung JK, Kang KW. Comprehensive gene expression analysis for exploring the association between glucose metabolism and differentiation of thyroid cancer. BMC Cancer. 2019;19(1):1260. doi: 10.1186/s12885-019-6482-7.
5. Roszik J, Ring KL, Wani KM, Lazar AJ, Yemelyanova AV, Soliman PT, et al. Gene expression analysis identifies novel targets for cervical cancer therapy. Front Immunol. 2018;9:2102. doi: 10.3389/fimmu.2018.02102.
6. Boland MR, Al-Maksoud A, Ryan É J, Balasubramanian I, Geraghty J, Evoy D, et al. Value of a 21-gene expression assay on core biopsy to predict neoadjuvant chemotherapy response in breast cancer: systematic review and meta-analysis. Br J Surg. 2021;108(1):24-31. doi: 10.1093/bjs/znaa048.
7. Rahmati Y, Mollanoori H, Kakavandi N, Nateghian A, Sayyahfar S, Babaei V, et al. Gene expression analysis in Kawasaki disease; bioinformatics and experimental approach. Inform Med Unlocked. 2020;20:100423. doi: 10.1016/j.imu.2020.100423.
8. Krokidis MG. Identification of biomarkers associated with Parkinson's disease by gene expression profiling studies and bioinformatics analysis. AIMS Neurosci. 2019;6(4):333-45. doi: 10.3934/Neuroscience.2019.4.333.
9. Porter TM, Hajibabaei M. MetaWorks: a flexible, scalable bioinformatic pipeline for high-throughput multi-marker biodiversity assessments. PLoS One. 2022;17(9):e0274260. doi: 10.1371/journal.pone.0274260.
10. Shen S, Kong J, Qiu Y, Yang X, Wang W, Yan L. Identification of core genes and outcomes in hepatocellular carcinoma by bioinformatics analysis. J Cell Biochem. 2019;120(6):10069-81. doi: 10.1002/jcb.28290.
11. Zhong J, Tang C, Peng W, Xie M, Sun Y, Tang Q, et al. A novel essential protein identification method based on PPI networks and gene expression data. BMC Bioinformatics. 2021;22(1):248. doi: 10.1186/s12859-021-04175-8.
12. Rezaei-Tavirani M, Rezaei Tavirani M, Zamanian Azodi M, Moravvej Farshi H, Razzaghi M. Evaluation of skin response after erbium:yttrium-aluminum-garnet laser irradiation: a network analysis approach. J Lasers Med Sci. 2019;10(3):194-9. doi: 10.15171/jlms.2019.31.
13. Joly F, Deret S, Gamboa B, Menigot C, Fogel P, Mounier C, et al. Photodynamic therapy corrects abnormal cancer-associated gene expression observed in actinic keratosis lesions and induces a remodeling effect in photodamaged skin.

J Dermatol Sci. 2018. doi: 10.1016/j.jdermsci.2018.05.002.
14. Padilla RS, Sebastian S, Jiang Z, Nindl I, Larson R. Gene expression patterns of normal human skin, actinic keratosis, and squamous cell carcinoma: a spectrum of disease progression. Arch Dermatol. 2010;146(3):288-93. doi: 10.1001/archdermatol.2009.378.
15. Ra SH, Li X, Binder S. Molecular discrimination of cutaneous squamous cell carcinoma from actinic keratosis and normal skin. Mod Pathol. 2011;24(7):963-73. doi: 10.1038/modpathol.2011.39.
16. Solus JF, Hassan K, Lee SJ, Hsi AC, Rosman IS, Dehmeri S, et al. Cutaneous squamous cell carcinoma progression is associated with decreased GATA-3 immunohistochemical staining. J Cutan Pathol. 2016;43(4):347-53. doi: 10.1111/cup.12667.
17. Wiegell SR, Wulf HC, Szeimies RM, Basset-Seguin N, Bissonnette R, Gerritsen MJ, et al. Daylight photodynamic therapy for actinic keratosis: an international consensus: International Society for Photodynamic Therapy in Dermatology. J Eur Acad Dermatol Venereol. 2012;26(6):673-9. doi: 10.1111/j.1468-3083.2011.04386.x.
18. Piaserico S, Mazzetto R, Sartor E, Bortoletti C. Combination-based strategies for the treatment of actinic keratoses with photodynamic therapy: an evidence-based review. Pharmaceutics. 2022;14(8):1726. doi: 10.3390/pharmaceutics14081726.
19. Grimm D, Bauer J, Wise P, Krüger M, Simonsen U, Wehland M, et al. The role of SOX family members in solid tumours and metastasis. Semin Cancer Biol. 2020;67(Pt 1):122-53. doi: 10.1016/j.semcancer.2019.03.004.
20. Wang P, Zhao Y, Fan R, Chen T, Dong C. MicroRNA-21a-5p functions on the regulation of melanogenesis by targeting SOX5 in mouse skin melanocytes. Int J Mol Sci. 2016;17(7):959. doi: 10.3390/ijms17070959.
21. Yuan WM, Fan YG, Cui M, Luo T, Wang YE, Shu ZJ, et al. SOX5 regulates cell proliferation, apoptosis, migration and invasion in KSHV-infected cells. Virol Sin. 2021;36(3):449-57. doi: 10.1007/s12250-020-00313-3.
22. Jerjes W, Upile T, Hamdoon Z, Mosse CA, Akram S, Hopper C. Photodynamic therapy outcome for oral dysplasia. Lasers Surg Med. 2011;43(3):192-9. doi: 10.1002/lsm.21036.
23. Pérez-Pérez L, García-Gavín J, Gilaberte Y. Daylight-mediated photodynamic therapy in Spain: advantages and disadvantages. Actas Dermosifiliogr (Engl Ed). 2014;105(7):663-74. doi: 10.1016/j.ad.2013.10.021.
24. Kwon N, Kim H, Li X, Yoon J. Supramolecular agents for combination of photodynamic therapy and other treatments. Chem Sci. 2021;12(21):7248-68. doi: 10.1039/d1sc01125a.